Optical observations of the very early phase GRB afterglows with MITSuME

Y. Yatsu,[1] H. Nakajima,[1] T. Enomoto,[1] K. Tokoyoda,[1] K. Kawakami,[1] N. Kawai[1], K. Asano,[1] T. Shimokawabe,[1] Y. A. Mori,[1] H. Endo,[1] D. Kuroda,[2] K. Yanagisawa,[2] M. Yoshida,[3] Y. Shimizu,[2] H. Toda,[2] S. Nagayama,[4] H. Hanayama,[5] and K. Ohta,[6]

[1] Tokyo Institute of Technology, 2-12-1, Oookayama, Meguro, Tokyo, 152-8551, Japan
[2] Okayama Astrophysical Observatory, 3037-5, Honjo, Kamogata, Asakuchi, Okayama 719-0232, Japan
[3] Hiroshima University, 1-3-1, Kagamiyama, Higashihiroshima, Hiroshima, 739-8526, Japan
[4] National Astronomical Observatory, 2-21-1, Oosawa, Mitaka, Tokyo, 181-8588, Japan
[5] Ishigaki Astronomical Observatory, 1024-1, Arakawa, Ishigaki, Okinawa, 907-0024, Japan
[6] Kyoto University, Kitashirakawaoiwake-cho, sakyo, Kyoto, 606-8502, Japan
E-mail(YY): yatsu@hp.phys.titech.ac.jp

Abstract

Optical observations of recent GRB afterglows are reported. Using The robotic telescope system *MITSuME* performed following observations prompted by GCN alerts and successfully obtained multicolor light-curves for four GRBs, 090426, 1208B, 100219A, and 100906A in these two years. Our observations revealed complicated and diverse light-curves. The light-curve of GRB090426 appears to be broken twice: a steepening break at $\sim$ 250 s and a flattening break at $\sim$ 1500 s after the trigger. In particular, the latter break is difficult to be explained by the standard model of GRB afterglows. On the other hand, the light-curve of GRB091218B shows a single power law decay as is expected by the standard model until 2100 s. The GRB100219A and GRB100906A show brightening phases just after the trigger that can be related with the onset of afterglows. In this study we summarize those observational results and possible interpretations.

Key words: gamma-rays: burst

1. Introduction

After the *HETE-II* era, the monitoring satellites for gamma-ray bursts (GRBs) enable the observations of very early stage of optical afterglows of GRBs during the prompt emissions. The observed light-curves revealed a huge variety of afterglow activity that may be reflecting the physical properties of the emitting regions. In order to constrain or understand the nature of the fireball itself, the immediate follow-up observations on several GRBs are required.

For this purpose we designed and constructed robotic observatories called *Multicolor Imaging Telescope for Survey and Monstrous Explosions* (hereafter *MITSuME*). We are operating two 50 cm diameter reflectors at Okayama Astrophysical Observatory (OAO/NAOJ) and Akeno Observatory (AO/ICRR) coupled with tricolor cameras capable with simultaneous three color (I_c, R_c, and g' bands) imaging observations using two pieces of dichroic mirrors and thanks to the high speed equatorial mount with a slew speed up to 9 deg s^{-1} (4 deg s^{-1} for AO), *MITSuME* can start observations within a few tens of seconds after the GCN alerts. *Murikabushi* 1 m diameter optical telescope in Ishigaki Astronomical Observatory (IAO) also possesses the same tricolor camera providing more deep images especially in the southern sky.

For these two years we have detected optical counterparts for 9 GRBs. In this paper we focus on the 4 bright GRBs (090426, 091208B, 100219A, and 100906A) for which we could successfully drew light-curves with $\sim$10 ks durations. As the preceding studies revealed, the obtained light-curves show a variety of activities, therefore, these phenomena are unlikely to be explained by an unified model at this moment. Thus here we show the multicolor light-curves and discuss each object separately.

2. Observations and Data Analysis

Fundamental properties of 4 GRBs we observed are summarized in Table 1. The delay of the follow-up observations is mainly due to the delivery time of GCN alert ($\sim 20s$) and the pointing time that depends on GRB coordinates. Fortunately, we could start observation within the prompt emission activity for 3 GRBs.

For the data reduction, a standard process, subtraction of dark frames and division by a flat frame, was applied to the obtained data sets. Then the flux of GRB afterglows were measured using aperture photometry technique. As the reference, the Guide Star Catalog (GSC) version 2.3 is employed for R_c and I_c bands. On the other hand, for g' band, the SDSS catalog is referred when that is available. In most cases, however, we convert g' magnitude from the GSC data following the conversion equation proposed by Sesar et al (2006).

3. Discussion (Results and Interpretations)

3.1. GRB090426

GRB090426 is the most distant short GRB discovered at $z = 2.61$ at this moment (Antonelli et al. 2009). The obtained multicolor light-curves are shown in Figure 1. Intriguingly the optical light-curves appear to be broken twice at $\sim$ 230 s and $\sim$ 1500 s after the trigger, while the X-ray emission declines with a single break at $\sim$ 230 s. Assuming the above interpretation we fitted the light curves with a double broken power-law function. The resultant parameters are summarized in Table 2.

At 230 s after the trigger, the optical and X-ray light-curves break simultaneously although the X-ray break is somewhat uncertain. The panchromatic phenomena can be explained by a jet break. Past observations have shown that the short GRBs tended not to show jet breaks as seen in the long GRBs, thus this result can be one of the evidences for the collimated outflow in short GRBs (Burrows et al. 2006). The second break at $\sim$ 1500 s is observed only in optical band. After the break, declining slope becomes flatter. This behavior is difficult to explain by the standard model.

A possible interpretation is the two component jet scenario (Racusin et al. 2008) in which the narrow jet component is dominant in the early phase of the afterglow and makes the jet break at 230 s, while in the later phase, the wide jet component becomes dominant exhibiting the flattening break. There could be another possibility, Xin et al. (2011) proposed that the flattening of the light-curve at $\sim$ 1500 s can be caused by the late energy injection. In order to examine those scenarios an investigation utilizing multi-wavelength SED is now undergoing (Nakajima et al. 2011 in preparation).

3.2. GRB091208B

The observation of GRB091208B was started at Akeno only 47 s after the *BAT* trigger, but was discontinued by bad weather. Then the OAO 50 cm telescope restarted observation at $\sim$ 600 s as shown in Figure 2. The gap of data points appear to be interpolated with a power-law function. The results of the model fitting with the

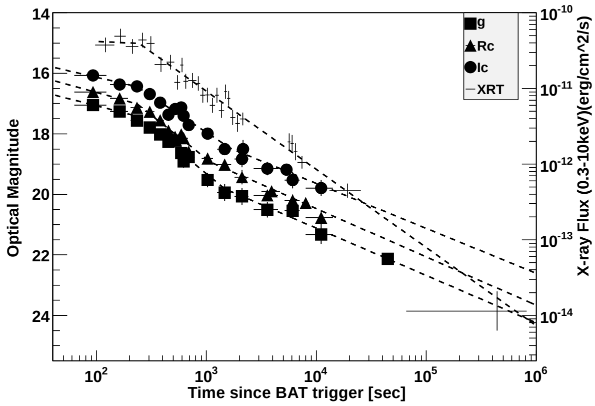

Fig. 1. X-ray and optical light-curves of GRB090426. The Cross marks shows X-ray flux measured by the *XRT*. The square, triangle and circle marks represent g', R_c, and I_c band, respectively. Dashed lines are the model functions. The best fit parameters are summarized in table 2

Table 2. Properties of light-curves of GRB090426.

Band	T_{break1} (s)	T_{break2} (s)
X	235 ± 59	—
g'	228 ± 14	1464 ± 6
R_c	233 ± 52	844 ± 549
I_c	252 ± 54	1528 ± 351

Band	α_1	α_2	α_3
X	0.08 ± 0.37	1.03 ± 0.05	—
g'	0.34 ± 0.12	1.21 ± 0.15	0.62 ± 0.08
R_c	0.34 ± 0.30	1.23 ± 0.16	0.67 ± 0.06
I_c	0.36 ± 0.15	1.01 ± 0.12	0.59 ± 0.11

above assumption is summarized in Table 3. In contrast prominent features are seen after 3000 s. In X-rays, there is also a gap of observations from $\sim$500 s to $\sim$6000 s.

Based on the standard model (Sari et al. 1998) the spectral index of radiating electrons can be constrained by the decay indices. Assuming that a cooling break exists between X-rays and optical band, the spectral index of electrons emitting X-rays can be expressed by $p_{\mathrm{X}} = (4\alpha_{\mathrm{X}} + 2)/3 \sim 2.0$. While, in optical band, the spectral index is $p_{\mathrm{opt}} = (4\alpha_{\mathrm{opt}} + 3)/3 \sim 2.0$, that is consistent with the value from the X-ray data.

On the other hand, the *XRT* can also provide the photon index independently, however, the observational gap prevents direct comparison. Alternatively we adopted the spectral photon index observed in the time interval of 5310 s $< t <$ 46280 s, $\Gamma_{\mathrm{X}} = 2.09 \pm 0.14$, that corresponds to $p_{\mathrm{X}} \sim 2.18$. These results indicate that the observed X-ray and optical photons are emitted from the same origin.

Table 1. Summary of GRBs detected by the *MITSuME* telescopes.

GRB	Redshift (z)	T_{90} (s)	$E_{\rm p}$ (keV)	$E_{\rm i}$ (ergs)	$T_{\rm start}$ [a] (s)	Observatory[b]
GRB090426	2.61	1.2	9^{+25}_{-8}	5×10^{51}	63	O
GRB091209B	1.06	14.5	144^{+18}_{-14}	—	47	A, O
GRB100219A	4.67	18.8	> 58	—	104	A
GRB100906A	1.73	114.4	180^{+45}_{-40}	2.2×10^{53}	26	A, O, I

[a] $T_{\rm start}$ is start time of optical observations from the *BAT* trigger.
[b] "A": Akeno-50cm, "O": Okayama-50cm, "I": Ishigaki Astronomical Observatory (1 m).

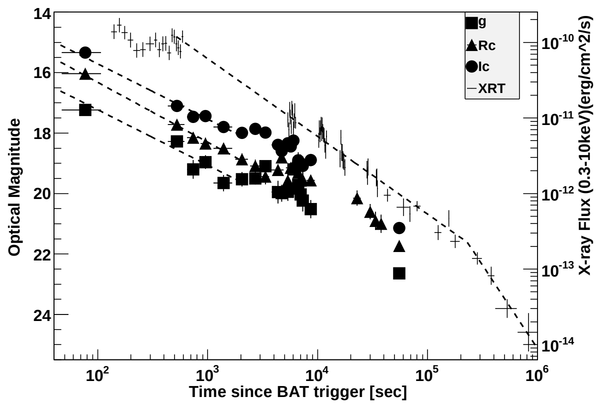

Fig. 2. X-ray and optical light-curves of GRB091208B. The Cross marks shows X-ray flux measured by the *XRT*. The circle, triangle and square marks represent g', R_c, and I_c data, respectively.

Table 3. Decay index of light-curves of GRB091208B before 2100 s from the trigger.

Band	α
X	1.03 ± 0.02
g'	0.76 ± 0.15
R_c	0.79 ± 0.10
I_c	0.74 ± 0.08

3.3. GRB100219A

GRB100219A has a comparatively high redshift of $z = 4.67$, that is the most distant GRB observed by *MITSuME* 50 cm telescopes. The light-curves of optical and X-ray energy bands are shown in Figure 3. Because of the Lyman-drop effect, we could not detected the optical counterpart in R_c and g' bands. The most intriguing feature is the brightening phase continuing until 1000s after the prompt emission. After the peak the light-curve shows power-law decay. The inices and peak time of the light-curves are summarized in Table 4.

The open question is what the brightening phase in the optical light-curve is. The first hypothesis is the $\nu_{\rm min}$ peak crossing the observed energy band. If that is the case, the brightening time index α_1 should be -0.5 and 0 for the circumstellar environments of the uniform ISM and the wind model distribution, respectively. Consequently, these values are rather small than the observed index.

Another hypothesis is that the optical peak represents the onset of the afterglow. In this case, the brightening index also depends on the distribution of the ISM, the indices should be -3 and $-1/3$ for the ISM model and the wind model, respectively. The observed index of $\alpha_1 = -0.85$ is the intermediate value between these models.

Assuming the observed peak is caused by the onset of afterglow, the initial Lorentz factor can be constrained. Based on Panaitescu & Kumar (2000) and Meszaros (2006), we have

$$\begin{aligned} \Gamma\left(t_{\rm peak}\right) &= \left[\frac{3E_\gamma(1+z)}{32\pi n m_{\rm p} c^5 \eta t_{\rm peak}^3}\right] \\ &= 84 E_{53}^{1/8} \eta_{0.2}^{-1/8} n_0^{-1/8}, \end{aligned} \tag{1}$$

where $E_\gamma = 10^{53} E_{53}$ erg is the isotropic-equivalent energy, $n = n_0$ cm^{-3} is the number density of the ISM, and $\eta = 0.2\eta_{0.2}$ is the radiative efficiency (from Bloom et al. 2003). Although the above estimation still contains some uncertainties, the obtained Lorentz factor is somewhat smaller than that expected for the usual GRBs (Molinari et al. 2007).

3.4. GRB100906A

GRB100906A may be the another candidate of GRB showing the onset of afterglow. For this GRB we started observation only 26 s after the *BAT* trigger. On the first two frames the afterglow was brightening in the all three colors. The model fitting adopting a broken power-law yielded a peak time of ~ 150 s. After that the afterglow decays as a power-law function. The model parameters

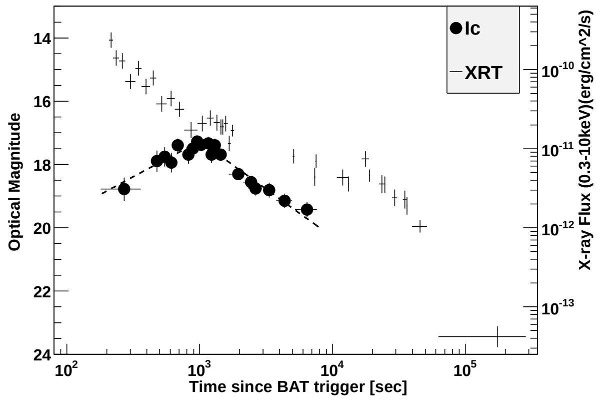

Fig. 3. X-ray and optical light-curves of GRB100219A. The Cross marks shows X-ray flux measured by the *XRT*. The circle, triangle and square marks represent g', R_c, and I_c data, respectively.

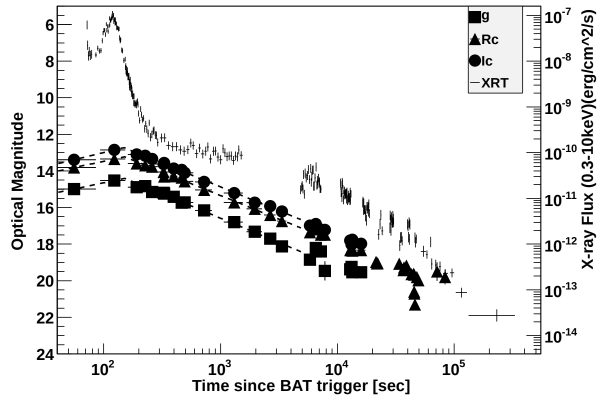

Fig. 4. X-ray and optical light-curves of GRB100906A. The Cross marks shows X-ray flux measured by the *XRT*. The circle, triangle and square marks represent g', R_c, and I_c data, respectively.

Table 4. Properties of light-curves of GRB100219A.

Band	$T_{\rm peak}$ (s)	α_1	α_2
I_c	1043 ± 80	-0.85 ± 0.29	1.22 ± 0.15

Table 5. Properties of light-curves of GRB100906A.

E	$T_{\rm break}$(s)	α_1	α_2
g'	153 ± 19	-0.54 ± 0.30	1.07 ± 0.05
R_c	152 ± 13	-0.54 ± 0.21	1.03 ± 0.04
I_c	149 ± 18	-0.62 ± 0.34	1.04 ± 0.04

are summarized in Table 5. The observed variability is obviously panchromatic as shown in Figure 4, indicating that the brightening can be caused by the onset of afterglow, rather than the $\nu_{\rm min}$ peak.

MITSuME data was taken with a fixed exposure time of 60 s, that is not sufficient to resolve the fast variability in early stages of the afterglows, therefore the brightening index contains large uncertaities, -0.5 ± 0.5. [1] . Nevertheless, the obtained upper limit is still smaller than that predicted by the ISM model (~ -3) and is likely to be the wind model ($\sim -1/3$).

For the GRB the initial Lorentz factor can be constrained as discussed above,

$$\Gamma\left(t_{\rm peak}\right) = 160 \eta_{0.2}^{-1/8} n_0^{-1/8}, \tag{2}$$

adopting the isotropic energy of $E_{\rm iso} \sim 2.2 \times 10^{53}$ erg reported by Golenetskii et al. (2010).

4. Conclusions

Here we reported the recently observed early phase GRB afterglows with *MITSuME*. GRB090426 shows complicated light-curves with double break, a panchromatic steepening break at 230 s and a flattening break at 1500 s after the trigger. To explain the light-curves the two-component jet model with a narrow jet and a wide jet is proposed. In contrast, the afterglow of GRB091208B shows a simple power-law decay until 2100s after the trigger. Comparison between the decay indices and the spectral indices indicates that the X-ray and optical radiation of the afterglows have the same origin, consistent with the standard model. Both GRB100219A and GRB100906A show brightening phases at the beginning of the afterglows with peaks at $\sim$ 1000 s and $\sim$ 150 s, respectively. The observed brightening time indices and the SED indicate that these phenomena can be explained by the onset of afterglows.

*1 Gorbovskoy et al. (2010) reported the results of *Master* observation with short exposure interval that indicates that the brightening curve seems to be steeper than our results.

References

Antonelli et al., 2009 A&A, 507, L45
Bloom et al., 2003 ApJ, 594, 674
Burows et al., 2006 ApJ., 653, 468
Golenetskii et al., 2010 GCN circular No. 11251
Gorbovskoy et al., 2010 GCN circular No. 11231
Nakajima et al., 2011 in preparation
Meszaros, 2006 Rep. Progr. Phys., 69, 2259
Molinali et al., 2007 A&A., 469, L13
Panaitescu & Kumar, 2000 ApJ., 543, 66
Racusin et al., 2008 Nature, 455, 183
Sari et al., 1998 ApJ., 497, L17
Sesar et al., 2006 AJ., 131, 2801
Xin et al., 2011 NMRAS., 410, 27